Interference and Throughput Analysis of Uplink User-Assisted Relaying in Cellular Networks

Hussain Elkotby and Mai Vu

Department of Electrical and Computer Engineering, Tufts University, Medford, MA, USA

Emails: Hussain.Elkotby@Tufts.edu, Mai.Vu@Tufts.edu

Abstract—**Relay-aided cooperative communication is a critical component of next generation cellular networks as it improves coverage and boosts system capacity. In this paper, we use stochastic geometry to study the performance of partial decode-and-forward (PDF) relaying through another idle user in uplink cellular communication. We analytically derive the average inter-cell interference power caused by system-wide deployment of this PDF relaying. This interference analysis provides the basis for quantitatively evaluating performance impacts of user-assisted relaying in cellular networks. We show that user-assisted relaying can significantly improve per-user transmission rate despite of increased inter-cell interference. This throughput gain further increases with higher idle-user density.**

Keywords- user-assisted relaying; partial decode-and-forward; stochastic geometry.

I. Introduction

Mobile operators driven by the increasing customer demand for new and better services place pressing requirements on the underlying wireless technologies to provide high data rates and wide coverage. Next generation networks that promise higher data rates and multifold increase in system capacity include 3GPP Long Term Evolution Advanced (LTE-A) and the emerging 5G systems. Ubiquitous coverage demands that services have to reach users in the most unfavorable channel conditions. An approach to improve performance in a poor coverage area is the use of relay-aided cooperative communication techniques. The latest release of the LTE standard allows the deployment of wireless relays to help the cell-edge mobiles.

Several modes of relay-aided communication have been proposed in the literature, including fixed relay station, mobile relay station, and using other user equipment (UE) as relay nodes [1]–[3]. Most existing results are derived for the first two modes of fixed and mobile relay stations. For example, simulation is used to compare the difference between relaying network architectures with mobile or fixed relay stations and contrast their performance gains in [1]. The resource allocation for uplink OFDMA-based cooperative relay networks has been studied in [2]. The third mode of relaying through other idle UEs (or user-assisted relaying) has only been studied through system simulations for decode-and-forward relaying in [3]. User-assisted relaying, nevertheless, provides more flexibility than fixed relaying in expanding the base station (BS) coverage into obscured areas especially where there is high density of idle UEs. The issue of battery power drainage of mobile UEs due to their cooperation in relaying other users data to the base station has also been examined through the emerging energy harvesting techniques [4]. In this paper, we analyze the performance of user-assisted relaying when deploying system-wide in a cellular network.

For cellular network analysis, stochastic geometry has been shown to be analytically tractable and capture some of the main performance trends. Stochastic geometry is used to develop a tractable model for downlink heterogeneous cellular networks which is comparable to the grid model and actual 4G deployment data in [5]. This model is further used to analyze downlink coordinated multipoint beamforming in which each user equipped with a single antenna can be served by either one or two base stations connected over backhaul links of infinite capacity in [6]. A user decides whether to connect to one or two base stations based on geometric policies taking into account its relative distances to the two closest base stations. In [7], Poisson spatial distribution is used to develop an analytic interference model for multi-cell multiple-input multiple-output cellular networks and derive its downlink average capacity.

Stochastic geometry is also used to analyze the performance of decode-and-forward relaying techniques in uplink cellular networks under the specific setting of a fixed number of relays deployed at a fixed distance from the BS with equal angular separation in each cell in [8].

In this paper, we study the performance of a partial decode-and-forward (PDF) relaying scheme in uplink cellular networks modeled using stochastic geometry. We consider the policy where each active UE selects the closest idle UE to relay its message to the destination and we assume that all nodes are equipped with a single antenna. We provide the geometric basis for a rigorous analysis of performance metrics such as outage probability or the throughput for the whole cellular system in contrast to the standalone analysis in [9]. We show that user-assisted relaying is able to achieve on the average 15% throughput gain over direct transmission when the density of idle UEs is twice that of the active UEs. This gain increases with higher density of idle users.

This paper is organized as follows: Section II describes the system model and the considered relaying scheme. Section III describes the network geometric model. Section IV provides the interference analysis and the derivation of cooperation probability. Then, Section V shows the numerical results. Finally, Section VI presents our conclusion.

II. System Description

A. System Overview

In this section, we give an overview of the system under consideration and the network description. We consider a cellular system which consists of multiple cells, each cell has a single base station and each base station serves multiple users.

Each of the users uses a distinct resource block, subsequently, no intra-cell interference is present. We assume that each user is served by the single base station that is closest to that user. Within this system, we study the impact on performance of the cooperation technique in which a user can partially relay its message to the base station through an idle user using the PDF relaying scheme described in Section II-C. In this work, we consider specifically the policy that the active user chooses the idle user that is closest to perform as a relay.

B. Relaying vs. Direct Transmission Channel Model

In this section we describe the channel model for the PDF relaying scheme proposed in [9] and show the modifications to account for the effects of interference in network deployment. We consider the relay channel shown in Fig. 1 in which a source $\mathcal{S}$ conditionally decides to exploit the help of a relay $\mathcal{R}$ to communicate a message to the destination $\mathcal{D}$ or directly convey its message to the destination, depending on the relative quality of the source-to-relay and source-to-destination links.

1) Physical Channel Model: In the relaying case, we use half-duplex time-division transmission over two phases with equal durations, and assume flat fading over the two phase period. We model the received signal at the ith relay and destination, respectively, during the first phase as

$$Y_{r,i}^b = h_{sr}^{(i)} x_{s,i}^b + I_{r,i}^b + Z_{r,i}^b \tag{1}$$

$$Y_{d,i}^b = h_{sd}^{(i)} x_{s,i}^b + I_{d,i}^b + Z_{d,i}^b \tag{2}$$

where b stands for broadcast transmission where the source broadcasts to both the relay and destination. The signals $x_{s,i}^b$ and $x_{s,i}^m$, are the transmitted codewords from the source in the first and second phase; $x_{r,i}^m$ is the transmitted codeword from the relay in the second phase; $I_{r,i}^b$ and $I_{d,i}^b$ represents the interference received at the ith relay and destination during the first phase; $Z_{r,i}^b$ and $Z_{d,i}^b$ are i.i.d $\mathcal{CN}(0,\sigma^2)$ that represent the noise at the ith relay and destination; and $h_{sr}^{(i)} = e^{j\theta_{i1}}|h_{sr}^{(i)}|$ and $h_{sd}^{(i)} = e^{j\theta_{i2}}|h_{sd}^{(i)}|$ are the complex channel gains that captures both the small and large scale fading of the source-to-relay and source-to-destination channels with uniformly distributed phases θ_{i1} and $\theta_{i2} \sim \mathcal{U}[0,2\pi]$, respectively.

Also, we model the received signal at the ith destination during the second phase as

$$Y_{d,i}^m = h_{sd}^{(i)} x_{s,i}^m + h_{rd}^{(i)} x_{r,i}^m + I_{d,i}^m + Z_{d,i}^m \tag{3}$$

where m denotes multiple access transmission where both the source and the relay send information to the destination; $h_{rd}^{(i)} = e^{j\theta_{ir}}|h_{rd}^{(i)}|$ captures the small scale and path loss fading of the relay-to-destination channel with phase shift θ_{ir}; $I_{d,i}^m$ represents the interference received at the ith destination during the second phase, respectively; and $Z_{d,i}^m \sim \mathcal{CN}(0,\sigma^2)$ represents the noise at the ith destination.

In the direct transmission case, we model the received signal at the ith destination as

$$Y_{d,i} = h_{sd}^{(i)} x_{s,i} + I_{d,i} + Z_{d,i} \tag{4}$$

where $I_{d,i}$ represents the average interference received at the ith destination during the transmission period; and $Z_{d,i} \sim \mathcal{CN}(0,\sigma^2)$ represents the noise at the ith destination.
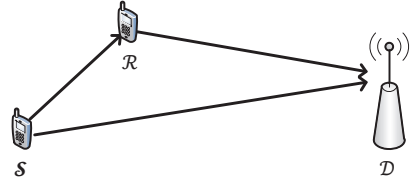

Fig. 1. Relay channel model

We assume that $I_{d,i}^b$, $I_{d,i}^m$, and $I_{d,i}$ have similar statistics and are independent of each other which is justified in Section III. Moreover, given the knowledge of all the nodes locations, we make use of the fact that interference at either the relay or destination is the sum of an infinite number of independent signals transmitted by an infinite number of sources that are distributed in the infinite 2-D plane and use the law of large numbers to approximate the interference as a complex Gaussian distribution. Also, since the transmitted codewords are realization of a complex Gaussian with zero mean, it is justified to set the first moment of interference to zero. To fully characterize interference as a complex Gaussian distribution, we derive the second moments of the terms $I_{d,i}^b$, $I_{d,i}^m \sim \mathcal{CN}(0,\sigma_d^2)$, and $I_{r,i}^b \sim \mathcal{CN}(0,\sigma_r^2)$ as an average over all the locations realizations of both active and relay nodes using tools of stochastic geometry in Section IV.

Also, the codeword $x_{s,i}^m = x_{s,i}^{m1} + x_{s,i}^{m2}$ represents the super-position of a common message codeword $x_{s,i}^{m1}$ and a private message codeword $x_{s,i}^{m2}$ which assume Gaussian distribution with zero mean and variances defined as follows:

$$\mathbb{E}\left[\left|x_{s,i}^m\right|^2\right] = \mathbb{E}\left[\left|x_{s,i}^{m1}\right|^2 + \left|x_{s,i}^{m2}\right|^2\right] = P_{s,i}^{m1} + P_s^{m2} = P_{s,i}^m,$$

$$\mathbb{E}\left[\left|x_{r,i}^m\right|^2\right] = P_{r,i}^m, \quad \mathbb{E}\left[\left|x_{s,i}^b\right|^2\right] = P_{s,i}^b, \quad \mathbb{E}\left[\left|x_{s,i}\right|^2\right] = P_{s,i}. \tag{5}$$

Moreover, the power allocation to each of the codewords has to satisfy the following constraints

$$\alpha_1 P_{s,i}^b + \alpha_2 P_{s,i}^m = P_{s,i}, \quad \alpha_2 P_{r,i}^m = P_{r,i}, \tag{6}$$

where $P_{s,i}$ and $P_{r,i}$ represent the total power allocated to the source and relay nodes within a single transmission period. α_1 and $\alpha_2 = 1 - \alpha_1$ represent the portions of the transmission time allocated to the first and second phases, respectively.

2) Model Reformulation into Standard Form: The aforementioned model in Section II-B1 in case of relaying can be reformulated to capture the effects of interference into the channel fading as follows

$$\tilde{Y}_{r,i}^b = \tilde{h}_{sr}^{(i)} x_{s,i}^b + \tilde{Z}_{r,i}^b, \quad \tilde{Y}_{d,i}^b = \tilde{h}_{sd}^{(i)} x_{s,i}^b + \tilde{Z}_{d,i}^b,$$

$$\tilde{Y}_{d,i}^m = \tilde{h}_{sd}^{(i)} x_{s,i}^m + \tilde{h}_{rd}^{(i)} x_{r,i}^m + \tilde{Z}_{d,i}^m, \tag{7}$$

where the new channel fading terms can be defined as

$$\tilde{h}_{sr}^{(i)} = \frac{h_{sr}^{(i)}}{\sqrt{\sigma_r^2 + \sigma^2}}, \quad \tilde{h}_{sd}^{(i)} = \frac{h_{sd}^{(i)}}{\sqrt{\sigma_d^2 + \sigma^2}}, \quad \tilde{h}_{rd}^{(i)} = \frac{h_{rd}^{(i)}}{\sqrt{\sigma_d^2 + \sigma^2}}, \tag{8}$$

and the equivalent noise terms $\tilde{Z}_{r,i}^b$, $\tilde{Z}_{d,i}^b$, and $\tilde{Z}_{d,i}^m$ are all i.i.d $\mathcal{CN}(0,1)$.

On the other hand, in the direct transmission case, the received signal at the ith destination during the whole transmission period can be remodeled as

$$\tilde{Y}_{d,i} = \tilde{h}_{sd}^{(i)} x_{s,i} + \tilde{Z}_{d,i}, \tag{9}$$

where the new channel fading is assumed to be the same as for the relaying case due to the equivalent interference assumption and $\tilde{Z}_{d,i} \sim \mathcal{CN}(0,1)$ is the noise at the ith destination.

C. Relaying Scheme Description

In this section, we describe the half-duplex partial decode-and-forward (PDF) relaying scheme presented in [9]. In this scheme, each transmission block is divided into 2 phases. In each block, the source $\mathcal{S}$ uses superposition coding and splits its information into a cooperative part, $U_{s,i}^{b}$ sent in the 1st phase and $U_{s,i}^{m1}$ sent in the 2nd phase, and a private part $V_{s,i}^{m2}$ sent in the 2nd phase. The common and private parts are transmitted at rates C_1 and C_2, respectively. The relay $\mathcal{R}$ decodes $U_{s,i}^{b}$ in the 1st phase and sends $U_{r,i}^{m} = U_{s,i}^{m1}$ in the 2nd phase. At the end of the 2nd phase, the destination $\mathcal{D}$ utilizes the received signals in both phases to decode both parts using joint maximum likelihood (ML) decoding rule.

Using Gaussian signaling, $\mathcal{S}$ and $\mathcal{R}$ constructs their transmit signals in the 1st and 2nd phase, respectively, as follows

$$x_{s,i}^{b} = \sqrt{P_{s,i}^{b}}U_{s,i}^{b}, \quad x_{r,i}^{b} = \sqrt{P_{r,i}^{m}}U_{s,i}^{m1}, \tag{10}$$

$$x_{s,i}^{m} = \sqrt{P_{s,i}^{m1}}U_{s,i}^{m1} + \sqrt{P_{s,i}^{m2}}V_{s,i}^{m2}. \tag{11}$$

Using the ML decoding rule, we obtain the following achievable rate which ensures reliable decoding at $\mathcal{R}$ and $\mathcal{D}$:

$$R \leq \min(C_1 + C_2, C), \tag{12}$$

where

$$C_1 = \alpha_1 \log\left(1 + \left|\tilde{h}_{sr}^{(i)}\right|^2 P_{s,i}^{b}\right), C_2 = \alpha_2 \log\left(1 + \left|\tilde{h}_{sd}^{(i)}\right|^2 P_{s,i}^{m2}\right),$$

$$C = \alpha_1 \log\left(1 + \left|\tilde{h}_{sd}^{(i)}\right|^2 P_{s,i}^{b}\right) \tag{13}$$

$$+ \alpha_2 \log\left(1 + \left|\tilde{h}_{sd}^{(i)}\right|^2 P_{s,i}^{m2} + \left(\left|\tilde{h}_{sd}^{(i)}\right|\sqrt{P_{s,i}^{m1}} + \left|\tilde{h}_{rd}^{(i)}\right|\sqrt{P_{r,i}^{m}}\right)^2\right).$$

The proposal in [9] is to adapt the scheme to the channel configuration to obtain two transmission cases: Direct transmission whenever $|\tilde{h}_{sr}^{(k)}|^2 \leq |\tilde{h}_{sd}^{(k)}|^2$ and PDF relaying otherwise.

III. Network Geometric Model

In this section, we describe the geometric model of the uplink cellular network under study. We assume that the users that will contend for the same resource block causing interference on each other are distributed on a two-dimensional plane according to a homogeneous and stationary Poisson point process (p.p.p.) Φ_1 with intensity λ_1. We also assume that Φ_1 is independent of another p.p.p. Φ_2 with intensity λ_2 that represents the distribution of another set of UEs that are in an idle state and can participate in relaying the messages transmitted by UEs in Φ_1. Furthermore, under the assumption that each BS serves a single mobile in a given resource block, we follow the same approach in describing BSs distribution as proposed in [10] where each BS is uniformly distributed in the Voronoi cell of its served UE.

A. Out-of-Cell Interference Model

Using the system and relay scheme description in Section II, we can express out-of-cell interference at the destination and the relay, respectively, as follows

$$I_{d,i} = \sum_{k \neq i}\left[A_k h_{sd}^{(k,i)}x_{s,k}^{b} + (1 - A_k)(h_{sd}^{(k,i)}x_{s,k}^{m} + h_{rd}^{(k,i)}x_{r,k}^{m})\right]B_k$$

$$+ h_{sd}^{(k,i)}x_{s,k}(1 - B_k), \tag{14}$$

$$I_{r,i} = \sum_{k \neq i}\left[A_k h_{sr}^{(k,i)}x_{s,k}^{b} + (1 - A_k)(h_{sr}^{(k,i)}x_{s,k}^{m} + h_{rr}^{(k,i)}x_{r,k}^{m})\right]B_k$$

$$+ h_{sr}^{(k,i)}x_{s,k}(1 - B_k), \tag{15}$$

where the summation is over all the active users. Here, $h_{sd}^{(k,i)}$ and $h_{rd}^{(k,i)}$, respectively, are the channel fading from the kth UE in Φ_1 and the associated relaying UE in Φ_2 to the BS associated with the ith UE in Φ_1. $h_{sr}^{(k,i)}$ and $h_{rr}^{(k,i)}$, respectively, are the channel fading from the kth UE in Φ_1 and the associated relaying UE in Φ_2 to the relaying UE associated with the ith UE in Φ_1.

The Bernoulli random variable $A_k \sim \text{Bern}(\rho_1)$ captures the transmission phase of the kth UE in Φ_1 with probability ρ_1, where $A_k = 1$ is used to indicate that interference at the ith destination results from the kth UE transmission during the first phase, and $A_k = 0$ indicates that this interference results from the kth UE and its associated relay transmission during the second phase. Here we assume $\rho_1 = 0.5$ and $\alpha_1 = \alpha_2 = 0.5$ to make $I_{d,i}, I_{d,i}^{b}$, and $I_{d,i}^{m}$ have equivalent statistics.

$B_k \sim \text{Bern}(\rho_2)$ is another Bernoulli random variable that captures the transmission strategy of the kth UE in Φ_1 with success probability ρ_2 where $B_k = 1$ is used to indicate the kth UE decision to exploit the help of another idle UE and apply the relaying transmission strategy. The cooperation probability ρ_2 will be computed later in Section III-B.

The channel fading terms can be split into their small scale and path loss fading components as

$$\left|h_{sd}^{(i)}\right|^2 = g_{sd}^{(i)}\|\mathbf{z}_i\|_2^{-\alpha}, \quad \left|h_{sr}^{(i)}\right|^2 = g_{sr}^{(i)}\|\mathbf{y}_i\|_2^{-\alpha},$$

$$\left|h_{rd}^{(i)}\right|^2 = g_{rd}^{(i)}D^{-\alpha}, \quad \left|h_{sd}^{(k,i)}\right|^2 = g_{sd}^{(k,i)}\|\mathbf{z}_k\|_2^{-\alpha}, \tag{16}$$

$$\left|h_{sr}^{(k,i)}\right|^2 = g_{sr}^{(k,i)}\|\mathbf{z}_k - \mathbf{y}_i\|_2^{-\alpha}, \quad \left|h_{rd}^{(k,i)}\right|^2 = g_{rd}^{(k,i)}\|\mathbf{z}_k\|_2^{-\alpha},$$

$$\left|h_{rr}^{(k,i)}\right|^2 = g_{rr}^{(k,i)}\|\mathbf{z}_k - \mathbf{y}_i\|_2^{-\alpha}, \tag{17}$$

with

$$D^2 = \|\mathbf{z}_i\|^2 + \|\mathbf{y}_i\|^2 - 2\|\mathbf{z}_i\|\|\mathbf{y}_i\|\cos\psi_0, \tag{18}$$

where we use the law of cosines to obtain Eq. (18); $\mathbf{z}_k$ and $\mathbf{y}_i$ are vectors representing the 2-D locations of the UEs in Φ_1 and Φ_2, respectively; and $\psi_0 \sim \mathcal{U}[0 : 2\pi]$ is a uniform random variable that represents the angle between the two vectors $\mathbf{z}_i$ and $\mathbf{y}_i$ connecting the ith UE to its base station and relaying node, respectively. Note that in Eq. (17) we use the out-of-cell interference approximation and set the location of out-of-cell source interferer and its associated relay to be the same as also done in [6]. $g_{sd}^{(k,i)}, g_{rd}^{(k,i)}, g_{sr}^{(k,i)}$, and $g_{rr}^{(k,i)}$ are all $i.i.d. \sim \exp(1)$ and represent the channel small scale fading.

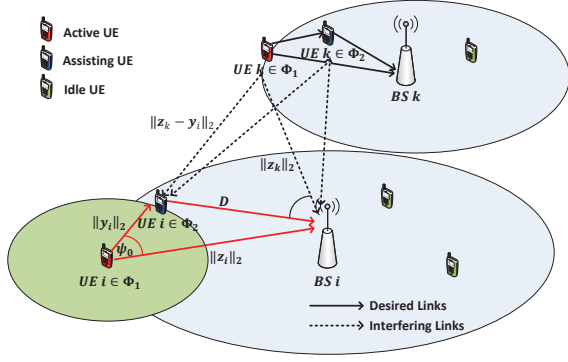Fig. 2.   System model

B. Cooperation Policies

We identify two cooperation policies E_1 and E_2 that defines whether a UE selects the relaying strategy or the direct transmission strategy. E_1 is an ideal policy that requires the active user to know the instantaneous channels to the closest idle user and to the base station, which can be defined according to the scheme described in [9] as

$$E_1 \quad = \left\{ \left| \tilde{h}_{sr}^{(k)} \right|^2 \geq \left| \tilde{h}_{sd}^{(k)} \right|^2 \right\} \tag{19}$$

$$\simeq \left\{ \frac{g_{sr} r_2^{-\alpha}}{\sigma_r^2} \geq \frac{g_{sd} r_1^{-\alpha}}{\sigma_d^2} \right\}, \tag{20}$$

where $r_1 = \|\mathbf{z}_i\|_2$ and $r_2 = \|\mathbf{y}_i\|_2$ which denote the source-to-destination and source-to-relay distances, respectively, as shown in Fig. 2. This event identifies whether an idle UE will be associated as a relay for the kth UE and participate in transmission, and hence cause interference.

In an interference limited scenario, we can ignore the effect of the noise variance σ^2 and hence follows Eq. (20) from which we can conclude that when the interference powers at the relay and at the destination are approximately the same, the cooperation event depends mainly on the distances from the source to relay and to the destination. Taking this fact into account and averaging out the effects of small scale fading, we identify a geometric cooperation policy E_2 as an approximate to the cooperation event in Eq. (20) as follows

$$E_2 \quad = \{r_1 \geq r_2, D \leq r_1\}. \tag{21}$$

Policy E_2 is more practical than policy E_1 in the sense that it only requires the active UE to know the distances to the nearest idle user and to the base station. It is worth noting that different network aided positioning techniques can be used by BSs to obtain information about UEs locations as surveyed in [11]. The extra condition $D \leq r_1$ ensures the elimination of all the cases that will result in an infinite interference at the relay. This approximation is also useful in simplifying the analysis to follow in Section IV. In the numerical results section, we will verify the validity of this approximation.

IV.   COOPERATION AND INTERFERENCE ANALYSIS

In this section, we analytically derive the cooperation probability and the average out-of-cell interference power at both the relay and destination.

A. Cooperation Probability

Here we analytically derive the cooperation probability for the geometric policy E_2. For the ideal policy E_1, analytical evaluation of the cooperation probability is complicated, hence we use numerical simulations instead, then incorporate the obtained probability into further analysis of system performance. We perform the analysis at a random BS assuming that it is associated with the ith UE. We assume that randomly picking this BS is equivalent to selecting a point uniformly distributed in the $\mathbb{R}^2$ plane as done in [10]. Under this assumption, the distribution of the distance r_1 between the ith UE and its associated BS can be shown to be Rayleigh distributed directly from the null probability of a two dimensional p.p.p. distribution.

Moreover, we can assume due to the stationarity of the Poisson point processes and the independence of Φ_2 from BSs distribution that the location of the UE associated with the BS under study represents the origin (typical) point of Φ_2. Then, each UE in Φ_1 chooses the closest UE in Φ_2 to assist it in relaying its message to the serving BS. Hence, similar to source-to-destination distance, the distribution of the source-to-relay distance r_2 between the ith UE and its associated relaying UE can be shown to be Rayleigh distributed directly from the null probability of a two dimensional p.p.p.. Thus, we have

$$\begin{aligned} f_{r_1}(r_1) &= 2\pi\lambda_1 r_1 e^{-\lambda_1 \pi r_1^2}, \\ f_{r_2}(r_2) &= 2\pi\lambda_2 r_2 e^{-\lambda_2 \pi r_2^2}. \end{aligned} \tag{22}$$

The probability of event E_2 in (21) which represents the cooperation probability ρ_2 can be evaluated as

$$\begin{aligned} \rho_2 &= \mathbb{P}\{E_2\} = \mathbb{P}\{r_1 \geq r_2, r_2 \leq 2r_1 \cos\psi_0\} \\ &= \int_{-\pi/2}^{-\pi/3} \mathcal{E}_1 d\psi_0 + \int_{\pi/3}^{\pi/2} \mathcal{E}_1 d\psi_0 + \int_{-\pi/3}^{\pi/3} \mathcal{E}_2 d\psi_0, \end{aligned} \tag{23}$$

where

$$\begin{aligned} \mathcal{E}_1 &= 2\pi\lambda_1\lambda_2 \int_0^\infty \int_0^{2r_1 \cos psi_0} r_1 r_2 e^{-\pi(\lambda_1 r_1^2 + \lambda_2 r_2^2)} dr_2 dr_1 \\ &= \frac{2\lambda_2 \cos^2 \psi_0}{\pi(\lambda_1 + 4\lambda_2 \cos^2 \psi_0)}, \end{aligned} \tag{24}$$

$$\begin{aligned} \mathcal{E}_2 &= 2\pi\lambda_1\lambda_2 \int_0^\infty \int_0^{r_1} r_1 r_2 e^{-\pi(\lambda_1 r_1^2 + \lambda_2 r_2^2)} dr_2 dr_1 \\ &= \frac{\lambda_2}{2\pi(\lambda_1 + \lambda_2)}, \end{aligned} \tag{25}$$

Substituting Eqs. (24) and (25) into Eq. (23), we obtain

$$\begin{aligned} \rho_2 &= \int_{-\pi/2}^{-\pi/3} \frac{2\lambda_2 \cos^2 \psi_0}{\pi(\lambda_1 + 4\lambda_2 \cos^2 \psi_0)} d\psi_0 \\ &+ \int_{\pi/3}^{\pi/2} \frac{2\lambda_2 \cos^2 \psi_0}{\pi(\lambda_1 + 4\lambda_2 \cos^2 \psi_0)} d\psi_0 + \frac{\lambda_2}{3(\lambda_1 + \lambda_2)}. \end{aligned} \tag{26}$$

B. Average Out-of-Cell Interference Power

To derive interference second moments, we first use the interference expression in Eq. (15) to express the interference power at the ith destination as in Eq. (27). $\theta_{k2,i}$ and $\theta_{kr,i}$ are realizations of independent and uniformly distributed random variables. We use the approximation described in [6] where

$$\mathcal{Q}_{d,i} = \sum_{k\neq i}\left[A_k\left|h_{sd}^{(k,i)}\right|^2 P_{s,k}^b + (1-A_k)\left(\left|h_{sd}^{(k,i)}\right|^2 P_{s,k}^m + \left|h_{rd}^{(k,i)}\right|^2 P_{r,k}^m + 2\left|h_{sd}^{(k,i)}\right|\left|h_{rd}^{(k,i)}\right|\sqrt{P_{s,k}^{m1}P_{r,k}^m}\cos\left(\theta_{k2,i}-\theta_{kr,i}\right)\right)\right]B_k$$
$$+ \left|h_{sd}^{(k,i)}\right|^2 P_{s,k}(1-B_k). \tag{27}$$

$$\mathcal{Q}_{d,i} = \sum_{k\neq i}\left[A_k\left|h_{sd}^{(k,i)}\right|^2 P_{s,k}^b + (1-A_k)\left(\left|h_{sd}^{(k,i)}\right|^2 P_{s,k}^m + \left|h_{rd}^{(k,i)}\right|^2 P_{r,k}^m\right)\right]B_k + \left|h_{sd}^{(k,i)}\right|^2 P_{s,k}(1-B_k). \tag{28}$$

$$\mathcal{L}_{\mathcal{J}_{d,i}}\left(s,\|\mathbf{z}_k\|_2\right) = \rho_2\left(\rho_1\mathcal{L}_G\left(s\|\mathbf{z}_k\|_2^{-\alpha}P_{s,k}^b\right) + (1-\rho_1)\mathcal{L}_G\left(s\|\mathbf{z}_k\|_2^{-\alpha}P_{s,k}^m\right)\mathcal{L}_G\left(s\|\mathbf{z}_k\|_2^{-\alpha}P_{r,k}^m\right)\right) + (1-\rho_2)\mathcal{L}_G\left(s\|\mathbf{z}_k\|_2^{-\alpha}P_{s,k}\right). \tag{30}$$

$$\mathcal{Q}_{r,i} = \sum_{k\neq i}\left[A_k\left|h_{sr}^{(k,i)}\right|^2 P_{s,k}^b + (1-A_k)\left(\left|h_{sr}^{(k,i)}\right|^2 P_{s,k}^m + \left|h_{rr}^{(k,i)}\right|^2 P_{r,k}^m\right)\right]B_k + \left|h_{sr}^{(k,i)}\right|^2 P_{s,k}(1-B_k). \tag{33}$$

interference is considered in expectation over the reception angles and since $\mathbb{E}_{\theta_{k2,i},\theta_{kr,i}}\left[\cos\left(\theta_{k2,i}-\theta_{kr,i}\right)\right]=0$, we can approximately rewrite the interference power at the ith destination as in Eq. (28). This approximation implies even though the out-of-cell source-relay pair transmits coherently (i.e. beamform) to its own destination, the two signals go through different fading channels to the cell under consideration and appear independent of each other.

Next, we use the Laplace transform of interference power to characterize the second moment of interference as

$$\mathcal{L}_{\mathcal{Q}_{d,i}}(s)=\mathbb{E}_{\mathcal{Q}_{d,i}}\left[e^{-s\mathcal{Q}_{d,i}}\right]$$
$$=\exp\left(-2\pi\lambda_1\int_{\|\mathbf{z}_i\|_2}^\infty\left(1-\mathcal{L}_{\mathcal{J}_{d,i}}\left(s,r\right)\right)r dr\right), \tag{29}$$

where the last equality follows from the *Laplace* functional expression for p.p.p. using polar coordinates; $\mathcal{L}_G(s)=1/(1+s)$ is the Laplace transform of an exponential random variable $G\sim\exp(1)$ and $\mathcal{L}_{\mathcal{J}_{d,i}}\left(s,\|\mathbf{z}_k\|_2\right)$ is expressed as in Eq. (30).

The second moment of interference at the destination can be computed from $\mathcal{L}_{\mathcal{Q}_{d,i}}(s)$ as follows

$$\sigma_d^2 = \mathbb{E}\left[\mathcal{Q}_{d,i}\right] = -\left.\frac{\partial\mathcal{L}_{\mathcal{Q}_{d,i}}(s)}{\partial s}\right|_{s=0} = \frac{2\pi\lambda_1\zeta}{\alpha-2}\|\mathbf{z}_i\|_2^{2-\alpha}, \tag{31}$$

where

$$\zeta = \rho_1\rho_2 P_{s,k}^b + \rho_2(1-\rho_1)\left(P_{r,k}^m + P_{s,k}^m\right) + (1-\rho_2)P_{s,k}. \tag{32}$$

Similarly, we can write the interference power at the ith idle UE as in Eq. (33) and its Laplace transform as in Eq. (34).

$$\mathcal{L}_{\mathcal{Q}_{r,i}}(s)=\exp\left(-\lambda_1\int_0^{2\pi}\int_{\|\mathbf{z}_i\|_2}^\infty\left(1-\mathcal{L}_{\mathcal{J}_{r,i}}\left(s,r,\theta\right)\right)r dr d\theta\right), \tag{34}$$

where $\mathcal{L}_{\mathcal{J}_{r,i}}\left(s,\|\mathbf{z}_k\|_2,\theta_k\right)$ is defined as in Eq. (35) in the following page. The term $\|\mathbf{z}_k-\mathbf{y}_i\|_2$ can be written in terms of $\|\mathbf{z}_k\|_2$ and θ_k using the law of cosines and the distance D defined in Eq. (18) as

$$\|\mathbf{z}_k-\mathbf{y}_i\|_2^2 = \|\mathbf{z}_k\|_2^2 + D^2 - 2\|\mathbf{z}_k\|_2 D\cos\theta_k. \tag{36}$$

Then, we can write the second moment of interference at the idle UE acting as a relay as follows

$$\sigma_r^2=\mathbb{E}\left[\mathcal{Q}_{r,i}\right] = -\left.\frac{\partial\mathcal{L}_{\mathcal{Q}_{r,i}}(s)}{\partial s}\right|_{s=0}$$
$$=\lambda_1\zeta\int_0^{2\pi}\int_{\|\mathbf{z}_i\|_2}^\infty\left(r^2 + D^2 - 2rD\cos\theta\right)^{-\alpha/2}r dr d\theta, \tag{37}$$
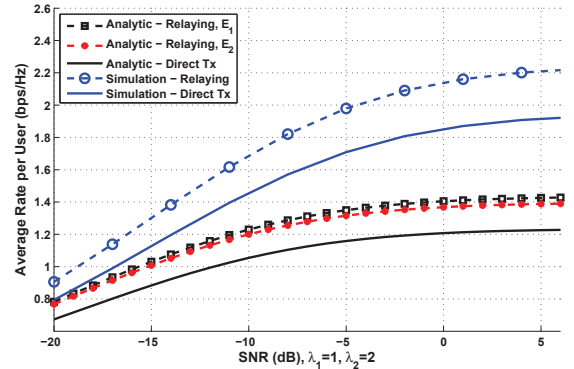
where ζ is defined as in Eq. (32).

Fig. 3. Comparison of average rates vs. SNR, $\lambda_1 = 1$, $\lambda_2 = 2$
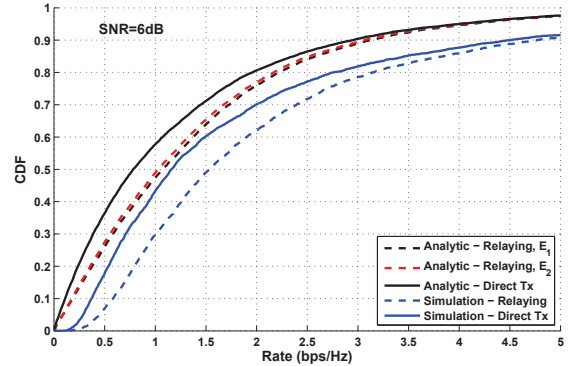

Fig. 4. Rate cumulative distribution function at SNR$= 6dB$, $\lambda_1 = 1$, $\lambda_2 = 2$

V. NUMERICAL RESULTS

In this section, we present the numerical results where we use $\lambda_1 = 1$; $P_{s,i} = P_{r,i}$; $P_{s,i}^b = P_{s,i}^m$; and $P_{s,i}^{m1}$ and $P_{s,i}^{m2}$ are numerically allocated optimally to maximize the rate. We use the average rate as a performance metric. We note that the expressions in (13) are convex in the interference powers, which are random based on active and relay users locations. For our analytic results we use the expected value of the interference powers to evaluate these rate expressions, while in simulation we take the expected value after evaluating the rate expressions for each set of locations and fading channels. Hence, we expect the analytic results to be a lower bound to the simulation results. This is shown in the average rate per user in Fig. 3 and the rate cumulative distribution function in Fig. 4. This gap between simulation and analytic results is tremendously improved in our future work by considering the first two moments of interference power distribution in analysis instead of only its mean. We also show in Figs. 3 and 4 that the results of the average rate per user in the network when

$$\mathcal{L}_{\mathcal{J}_{r,i}}\left(s,\|\mathbf{z}_k\|_2,\theta_k\right) = \rho_2\left(\rho_1\mathcal{L}_G\left(s\|\mathbf{z}_k-\mathbf{y}_i\|_2^{-\alpha}P_{s,k}^b\right)+(1-\rho_1)\mathcal{L}_G\left(s\|\mathbf{z}_k-\mathbf{y}_i\|_2^{-\alpha}P_{s,k}^m\right)\mathcal{L}_G\left(s\|\mathbf{z}_k-\mathbf{y}_i\|_2^{-\alpha}P_{r,k}^m\right)\right)$$
$$+ (1-\rho_2)\mathcal{L}_G\left(s\|\mathbf{z}_k-\mathbf{y}_i\|_2^{-\alpha}P_{s,k}\right), \tag{35}$$
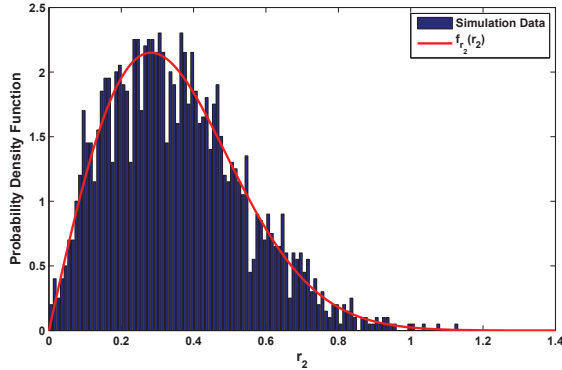
Fig. 5. Cooperation link distance, r_2, distribution validation

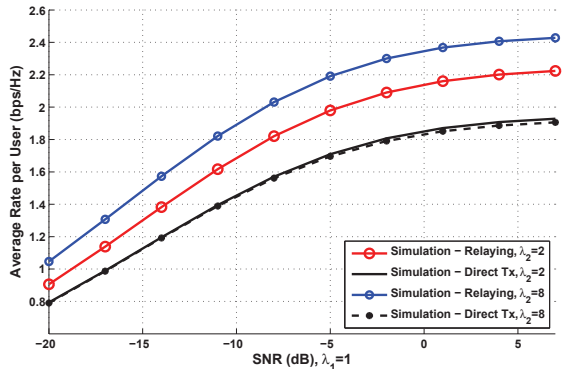Fig. 7. Cooperation event probability vs. the density of idle UEs

Fig. 6. Comparison of average rates vs. SNR, $\lambda_1 = 1$, $\lambda_2 = \{2, 8\}$

analysis provides the basis for evaluating system performance metric such as outage, coverage and throughput. Numerical results verify our analysis and show that user-assisted relaying can significantly improve the per-user transmission rate, despite increased out-of-cell interference. The throughput gain increases with higher idle user density.

using the geometric cooperation policy E_2 in (21) approaches that of the ideal cooperation policy E_1 in (20) which validates our choice of E_2.

In Fig. 5, we validate our choice of the Rayleigh distribution to model the distance r_2 of the source-to-relay link where $\lambda_2 = 2$. In Fig. 6, we compare the average rate per user of the PDF relaying scheme to the direct transmission when we increase the idle UEs density from $\lambda_2 = 2$ to $\lambda_2 = 8$. It shows that the throughput gain increases substantially (from 15% to 24%) by increasing the idle user density. This improvement can also be observed through the increase in cooperation probability in Fig. 7. Note that in our setup, each UE selects the closest idle UE to act as a relay without considering the relay-to-destination link quality. Hence the potential performance gain via relaying can increase further when taking into account specific link qualities. Also the rates shown in Figures 3 and 6 are averaged over all locations of both the active and relay users; the specific rate gain varies with location and can be significantly higher for certain parts of the cell.

VI. CONCLUSION

In this paper, we analyze system-wide performance impact of deploying user-assisted partial decode-and-forward relaying in a cellular network. Using a stochastic geometry model for user and base station locations, we analytically derive the cooperation probability and the average interference power generated to the relayed user and destination base station. This
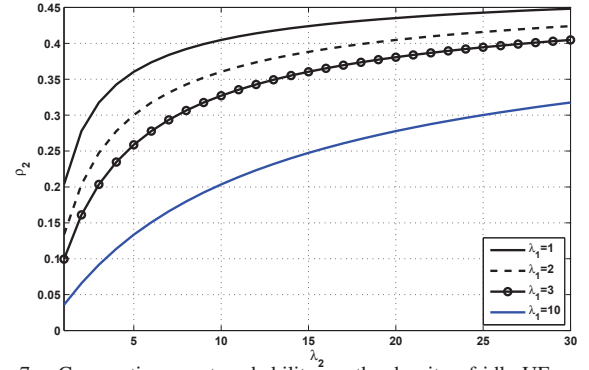
REFERENCES

[1] Nourizadeh, H.; Nourizadeh, S.; Tafazolli, R., "Performance Evaluation of Cellular Networks with Mobile and Fixed Relay Station," Vehicular Technology Conference, 2006. VTC-2006 Fall. 2006 IEEE 64th , vol., no., pp.1,5, 25-28 Sept. 2006

[2] Odeh, N.; Abolhasan, M.; Safaei, F., "Low Complexity Interference Aware Distributed Resource Allocation for Multi-Cell OFDMA Cooperative Relay Networks," Wireless Communications and Networking Conference (WCNC), 2010 IEEE , vol., no., pp.1,6, 18-21 April 2010

[3] Vanganuru, K.; Puzio, M.; Sternberg, G.; Shah, K.; Kaur, S., "Uplink system capacity of a cellular network with cooperative mobile relay," Wireless Telecommunications Symposium (WTS), 2011 , vol., no., pp.1,7, 13-15 April 2011

[4] Krikidis, Ioannis, "Simultaneous Information and Energy Transfer in Large-Scale Networks with/without Relaying," Communications, IEEE Transactions on , vol.62, no.3, pp.900,912, March 2014

[5] Andrews, J.G.; Baccelli, F.; Ganti, R.K., "A Tractable Approach to Coverage and Rate in Cellular Networks," Communications, IEEE Transactions on , vol.59, no.11, pp.3122,3134, November 2011

[6] A. Giovanidis and F. Baccelli, "A Stochastic Geometry Framework for Analyzing Pairwise-Cooperative Cellular Networks," CoRR, vol. abs/1305.6254, 2013.

[7] X. Ge, K. Huang, C.-X. Wang, X. Hong, and X. Yang, Capacity analysis of a multi-cell multi-antenna cooperative cellular network with co-channel interference, IEEE Transactions on Wireless Communications, vol. 10, no. 10, pp.3298-3309, Oct. 2011.

[8] F. Librino and M. Zorzi, "Relaying Strategies for Uplink in Wireless Cellular Networks," CoRR, vol. abs/1306.6017, 2013.

[9] Abu Al Haija, A.; Vu, Mai, "A half-duplex cooperative scheme with partial decode-forward relaying," Information Theory Proceedings (ISIT), 2011 IEEE International Symposium on , vol., no., pp.1886,1890, July 31 2011-Aug. 5 2011

[10] Novlan, T.D.; Dhillon, H.S.; Andrews, J.G., "Analytical Modeling of Uplink Cellular Networks," Wireless Communications, IEEE Transactions on , vol.12, no.6, pp.2669,2679, June 2013

[11] Guolin Sun; Jie Chen; Wei Guo; Liu, K.J.R., "Signal processing techniques in network-aided positioning: a survey of state-of-the-art positioning designs," Signal Processing Magazine, IEEE , vol.22, no.4, pp.12,23, July 2005